

# Synthesis and Study of $\beta$ -Chlorhydrine and $\alpha$ -Chloroacid Ferroelectric Liquid-Crystal Derivatives

T. Sierra, E. Meléndez, and J. L. Serrano\*

Química Orgánica, Facultad de Ciencias, Instituto de Ciencia de los Materiales de Aragón, Universidad de Zaragoza—CSIC, 50009 Zaragoza, Spain

A. Ezcurra and M. A. Pérez-Jubindo

Departamento de Física Aplicada II, Facultad de Ciencias, Universidad del País Vasco, Apto. 644, 48080 Bilbao, Spain

Received July 30, 1990

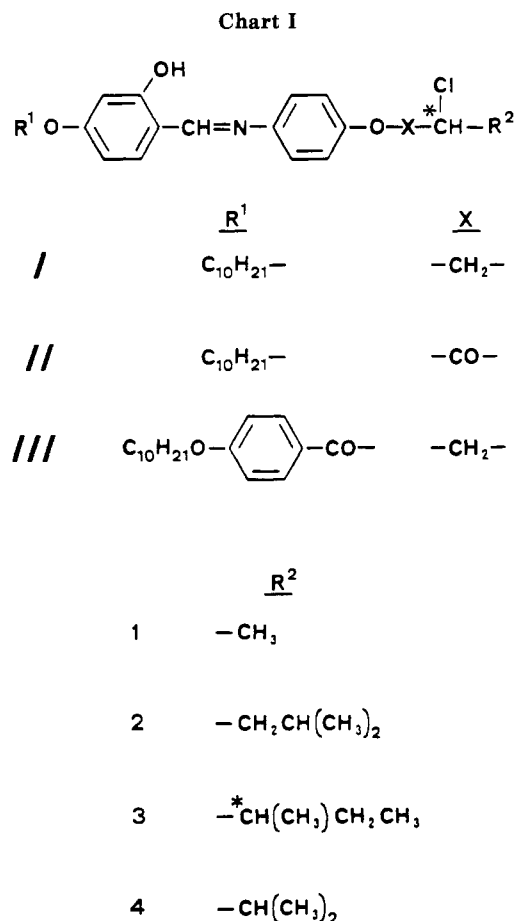
The synthesis and ferroelectric properties of three new series of chiral Schiff bases is presented. Series I, (4*R*\*)-*N*-(4-(decyloxy)-2-hydroxybenzylidene)anilines, have  $\beta$ -chlorhydrine derivatives of four  $\alpha$ -amino acids (alanine, leucine, isoleucine, and valine) as chiral tails. This series is used as a model, and we introduce two structural modifications in order to improve ferroelectric properties. In the compounds of series II we replaced the  $\beta$ -chlorhydrines with homologous  $\alpha$ -chloro amino acids as terminal chains. With the compounds in series III, (4*R*\*)-*N*-{4-(4'-(decyloxy)benzoyloxy)benzoyloxy}-2-hydroxybenzylidene}anilines, we introduce a third aromatic ring to obtain smectogenic properties. Eleven of the twelve compounds show the chiral SmC. The compounds in series III show the broadest ranges and the highest stability of the SmC phase. The spontaneous polarization (*P*<sub>s</sub>) values were measured in the pure compound. The highest values were obtained for the compounds in series II (48–130 nC/cm<sup>2</sup>).

## Introduction

The study of the relationship between molecular structure and ferroelectric properties is one of the most interesting subjects in liquid-crystal research.<sup>1,2</sup> In a previous paper<sup>3</sup> we describe some chiral Schiff bases derived from carbocyclic and heterocyclic aldehydes that exhibit ferroelectric behavior. Of these bases the 4-(decyloxy)-2-hydroxybenzaldehyde derivatives showed the greatest chemical stability when heated in the presence of electric fields. However those compounds with typical chiral tails (2-methylbutanol, 2-chloropropanol, etc.) have low *P*<sub>s</sub> values. The best results were obtained with (4*R*)-((2-chloropropyl)oxy)-*N*-(4-(decyloxy)-2-hydroxybenzylidene)aniline, which shows a *P*<sub>s</sub> value of 13 nC/cm<sup>2</sup>.

Starting from these previous results and to improve the ferroelectric properties of the compounds, we have synthesized three new series of mesogenic compounds (see Chart I).

These series have 2-hydroxybenzylideneaniline as a common mesogenic core. In series I we introduced other  $\beta$ -chlorhydrine chiral tails derived from  $\alpha$ -amino acids (L-leucine, L-isoleucine, L-valine besides L- $\alpha$ -aniline). With these terminal chains we expected to obtain higher *P*<sub>s</sub> values by increasing the size of the alkyl group linked to the chiral center.<sup>4-6</sup> In series II we replaced the  $\beta$ -chlorhydrines with their corresponding  $\alpha$ -chlorocarboxylic acids as chiral terminal tails; we followed the criterion that strong dipoles, as carbonyl groups near the asymmetric center, favor higher *P*<sub>s</sub> values.<sup>1,4,5</sup> In series III we incorporated a third aromatic ring to the core of the compounds in series I substituting the decyloxy group by 4-(decyloxy)benzoyloxy. The introduction of the third aromatic ring has been shown to give rise to wider SmC ranges in some chiral and achiral mesogenic compounds.<sup>7-10</sup> For



the sake of simplification, each compound is represented by a Roman number (I–III) and an Arabic (1–4) number corresponding to the series and terminal tail, respectively.

(1) Lagerwall, S. T.; Otterholm, B.; Skarp, K. *Mol. Cryst. Liq. Cryst.* **1987**, *152*, 503.

(2) Beresnev, L. A.; Blinov, L. M.; Osipov, M. A.; Pikin, S. A. *Mol. Cryst. Liq. Cryst.* **1988**, *158A*, 3.

(3) Barberá, J.; Meléndez, E.; Serrano, J. L.; Sierra, M. T. *Mol. Cryst. Liq. Cryst.* **1989**, *170*, 151.

(4) Bahr, C.; Heppke, G. *Mol. Cryst. Liq. Cryst. Lett.* **1986**, *4*(2), 31.

(5) Sakurai, T.; Mikami, N.; Higuchi, R.; Honma, M.; Ozaki, M.; Yoshino, K. *J. Chem. Soc., Chem. Commun.* **1986**, 978.

(6) Tinh, N. H.; Salleneuve, C.; Destrade, C. *Ferroelectrics* **1988**, *85*, 435.

(7) Takenaka, S.; Ikemoto, T.; Kusabayashi, S. *Bull. Chem. Soc. Jpn.* **1986**, *59*(12), 3965.

(8) Sakagami, S. *Bull. Chem. Soc. Jpn.* **1987**, *60*(3), 1153.

(9) Demus, D.; Demus, H.; Zschke, J. *Flüssige Kristalle in Tabellen*; VEB Deutscher Verlag für Grundstoffindustrie: Leipzig, 1974.

(10) Neubert, M. E.; Maurer, L. *J. Mol. Cryst. Liq. Cryst.* **1977**, *43*, 313.

Compounds I-1 and II-1 have been described in a previous paper.<sup>3</sup> However, both compounds were resynthesized for this work by using the same synthetic route as used for all other compounds in this paper. The thermal values for compound II-1 show some differences with respect to the published data due to the higher enantiomeric purity obtained this time.

## Results and Discussion

**Chemical Stability of the Schiff Bases.** In previous papers<sup>3,11</sup> we studied the stability of some ferroelectric liquid crystals Schiff base derivatives. The presence of a  $-\text{COCHClCHR}'$  group and the imine linkage in positions 1,4 of the aromatic ring, are not very stable at high temperatures. The loss of HCl giving rise to a conjugate structure<sup>12</sup> seems to be favored by the basic character of the nitrogen atom.

All the compounds in this paper showed a high degree of stability, which remained unchanged after several DSC scannings above their clearing points. The hydroxyl group in position 2 of the benzylidene ring plays an important role in the terminal stability of these compounds. This hydroxyl group forms a H bond with the nitrogen in the imine group. The energies of this bond were calculated for the compounds of the three series by using the method applied by Schaefer to the  $^1\text{H}$  NMR data<sup>13a</sup> (Table IIIa). The values obtained are  $39.7 \pm 0.8$  (series I),  $40.1 \pm 0.8$  (series II), and  $38.9 \pm 0.8$  kJ/mol (series III). These intramolecular H bonds are very strong and reduce the basic character of the nitrogen in the imine, thus stabilizing the structure.<sup>14</sup>

Slight decomposition was observed in compound II-1 when high temperatures were reached in the presence of an electric field. For this reason no  $\alpha$ -chlorocarboxylic acids were introduced in series III because of the high temperatures at which this mesogenic unit shows the SmC phase.

**Mesophase Characterization.** The mesophase were identified according to their textures, which were observed in the optical microscopy. The smectic C chiral mesophase of the (4*R*\*)-*N*-(4-(decyloxy)-2-hydroxybenzylidene)-anilines (series I and II) showed focal-conic and schlieren textures. The focal-conic textures in the  $\text{S}_{\text{C}}^*$  mesophase appears when the focal-conic texture of the  $\text{S}_{\text{A}}$  mesophase cools. The schlieren texture appears gradually from the  $\text{S}_{\text{A}}$  homeotropic texture obtained when the sample is submitted to mechanical stress.

The smectic C chiral mesophase of the (4*R*\*)-*N*-[4-(4'-(decyloxy)benzoyloxy)-2-hydroxybenzylidene]anilines in series III exhibited focal-conic, schlieren, and marbled textures. From the isotropic phase the cholesteric mesophase appears as an oily streak texture that on cooling gives rise to a focal-conic texture. Compound III-3 behaves differently. The cholesteric phase appeared from the isotropic liquid through a fingerprint-type texture that changed to a blurred-schlieren texture in the  $\text{S}_{\text{C}}^*$  phase. The mechanical stress of these last textures led to the formation of a marbled texture in both cases.

The three phases, Ch,  $\text{S}_{\text{A}}$ , and  $\text{S}_{\text{C}}$ , were confirmed by means of X-ray measurements in compounds I-4, II-2, II-4,

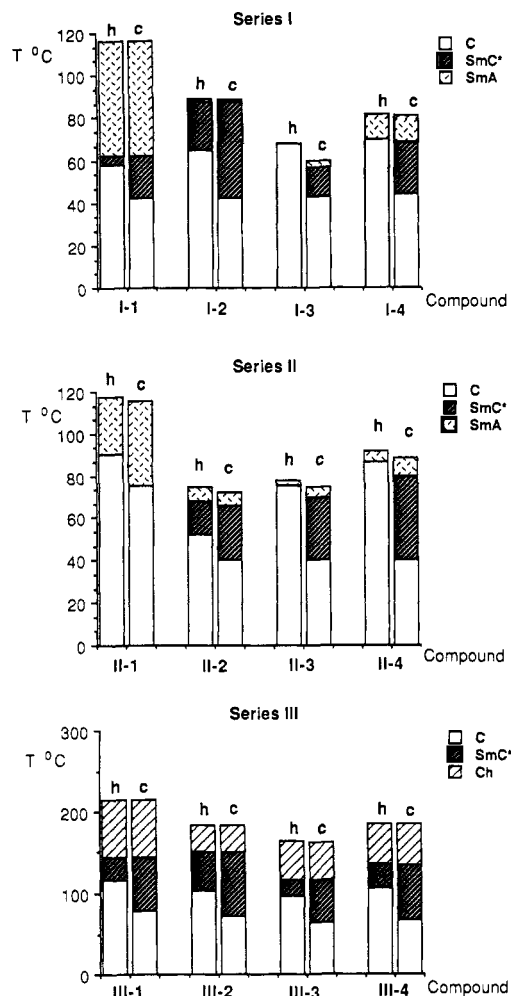


**Figure 1.** Transition temperatures of the compounds in series I, II, and III in the second heating (h) and cooling (c) processes.

and III-1. Magnetically orientated diffraction patterns were obtained by aligning the  $\text{S}_{\text{A}}$  mesophase under a magnetic field of 1.7 T and slow cooling into the  $\text{S}_{\text{C}}$  mesophase. Compound III-1, which does not show a  $\text{S}_{\text{A}}$  mesophase, could not be aligned. The interlayer spacing in the  $\text{S}_{\text{A}}$  and  $\text{S}_{\text{C}}$  phases was calculated from the low-angle diffraction maxima ( $2\theta = 3.0\text{--}3.4^\circ$ ). The data obtained indicate that in the  $\text{S}_{\text{C}}$  mesophase, the layer thickness is only slightly smaller (1 or 2 Å at most) than in the  $\text{S}_{\text{A}}$  mesophase and decreases gradually on decreasing the temperature. By comparing the layer thickness in the  $\text{S}_{\text{A}}$  and  $\text{S}_{\text{C}}$  phases, one estimates a maximum value for the tilt angle in the  $\text{S}_{\text{C}}$  phase between  $16^\circ$  and  $27^\circ$  depending on the compound.

**Mesogenic Properties.** The thermal data of the compounds of the three series are gathered in Table I.

All the compounds, except II-1, show the potentially ferroelectric  $\text{SmC}^*$  phase.

The compounds in series I and II show small ranges of  $\text{SmC}$  phase. Compound II-1 does not even show  $\text{SmC}$  behavior and in L-isoleucine and L-valine derivatives (compounds I-3, II-3 and I-4, II-4, respectively) this phase is monotropic. The seven compounds show the phase sequence I- $\text{SmA}$ - $\text{SmC}^*$ -C with the ferroelectric phase at temperatures lower than  $100^\circ\text{C}$  (Figure 1).

As can be seen in Figure 1, the widest  $\text{SmC}^*$  ranges appear in series III. Likewise, these compounds show important differences with regard to the compounds in series I and II: they exhibit a cholesteric phase above the  $\text{SmC}^*$  one and higher mesophase stabilities. These results

(11) Marcos, M.; Serrano, J. L.; Sierra, M. T.; Etxebarria, J.; Ezcurra, A. *Ferroelectrics* **1987**, *85*, 415.

(12) Barberá, J.; Omenat, A.; Serrano, J. L.; Sierra, M. T. *Liq. Crystall.* **1989**, *5*(6), 1775.

(13) (a) Schaefer, T. *J. Phys. Chem.* **1975**, *79*, 1888. (b)  $E$  (kcal/mol) =  $\Delta\delta + 0.4 \pm 0.2$ ,  $\Delta\delta = \delta_{\text{OH}} - \delta_{\text{OH-phenol}}$  in  $\text{CHCl}_3$ .  $\delta_{\text{OH-phenol}} = 4.59$  ppm.

(14) Elguero, J.; Jaime, C.; Marcos, M.; Meléndez, E.; Sánchez-Ferrando, F.; Serrano, J. L. *J. Mol. Struct. (THEOCHEM)* **1987**, *150*, 1.

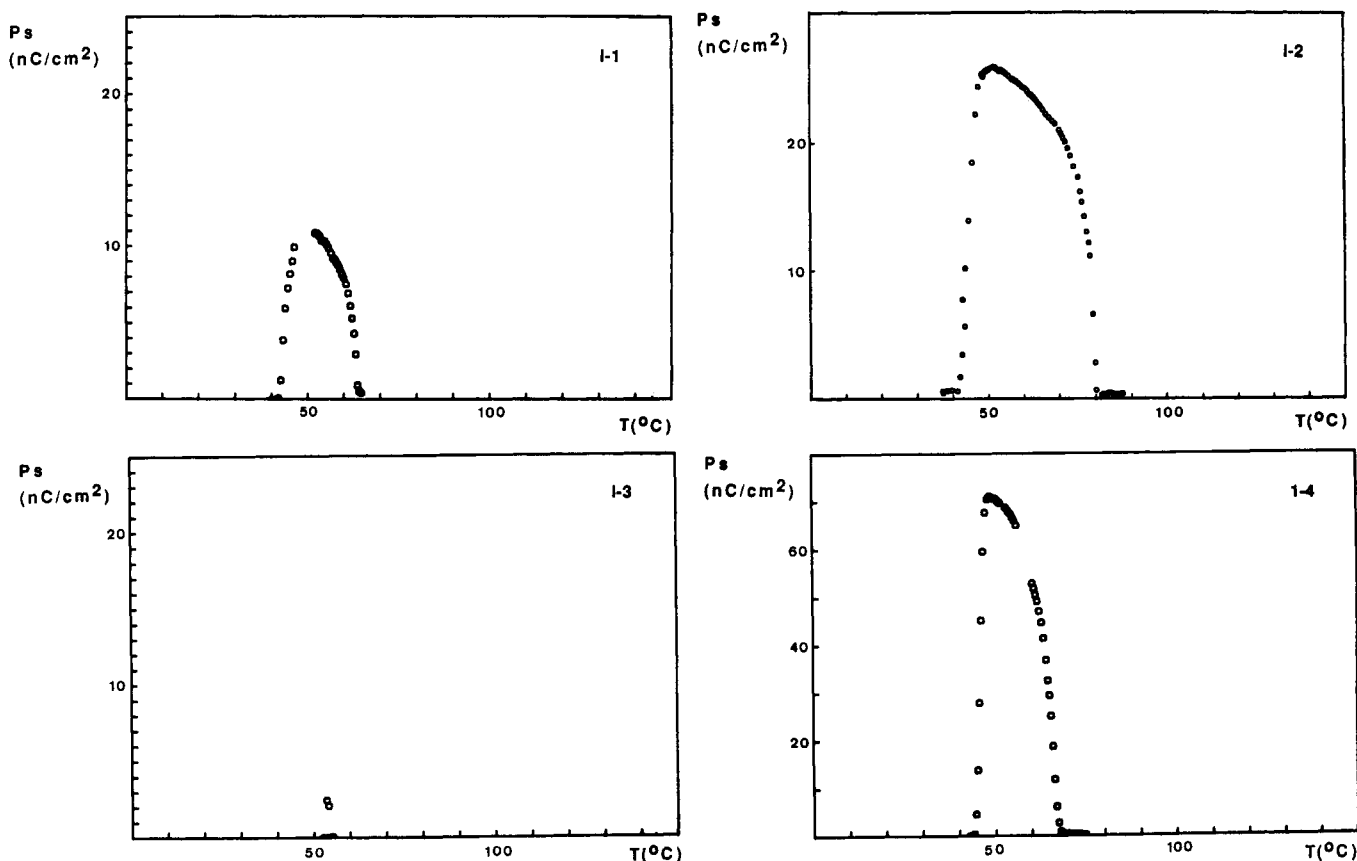


Figure 2. Temperature dependence of the polarization of the compounds in series I in the SmC\* phase.

Table I. Transition Temperatures (°C) and Enthalpies (kJ/mol, in Parentheses) for the Compounds in Series I-III

compd	C	→ S <sub>C</sub> * →	S <sub>A</sub>	→ Ch →	I
I-1	59.0 (9.9)		65.5 <sup>a</sup>		118.1 (1.4)
I-2	64.4 (5.6)		87.7 <sup>a</sup>		88.3 (2.4)
I-3	67.6 (11.7)		56.4 <sup>a</sup>		59.9 (0.7)
I-4	69.6 (6.6)		67.1 <sup>a</sup>		81.2 (0.8)
II-1	90.2 (9.3)				117.4 (1.3)
II-2	52.3 (3.6)		68.0 (0.02)		74.8 (1.1)
II-3	75.2 (8.3)		72.3 (0.03)		77.9 (0.8)
II-4	86.4 (8.1)		82.0 (0.03)		91.7 (0.9)
III-1	116.7 (8.2)		144.9 (0.1)		214.8 (0.3)
III-2	102.5 (6.7)		150.0 (0.5)		183.9 (0.3)
III-3	96.13 (6.1)		116.3 (0.2)		163.5 (0.2)
III-4	106.0 (7.3)		135.3 (0.4)		185.9 (0.3)

<sup>a</sup>Transition observed only by optical microscopy.

could be due to structural and electronic factors: The introduction of a third aromatic ring in the central core gives rise to a considerable elongation of the molecule, thus increasing the *L/D* relationship. This effect and an extension of the conjugation through the ester group cause a substantial increase in the anisotropy of the molecular polarizability. Consequently, intermolecular interactions are favored and the stability of the SmC\* phase is therefore increased. Moreover, the molecular dipole is modified because of the partial dipole moment associated with the ester linkage. In a previous paper<sup>15</sup> we evaluated this dipole by MNDO calculations using the methyl benzoate as a model. These results showed an important dipolar component parallel to the long molecular axis. This may explain<sup>16</sup> the appearance of nematic mesomorphism.

(15) Barberá, J.; Navarro, F.; Oriol, L.; Piñol, M.; Serrano, J. L. *J. Pol. Sci. Part A, Pol. Chem.* 1990, 28, 703.

(16) Barberá, J.; Marcos, M.; Serrano, J. L. *Mol. Cryst. Liq. Cryst.* 1987, 149, 225.

Table II. Saturation Ps Values (nC/cm<sup>2</sup>)

terminal tail	series		
	I	II	III
1	12		18
2	26	60	34.5
3	2.5	48	46
4	71	130	59

With regard to the chiral terminal tails, the widest smectic C ranges appear in the L-leucine derivatives in the three series (I-2, II-2, III-2). The elongation of the alkyl group from L-alanine derivatives increases the anisotropy of the polarizability, and as a consequence of the SmC phase is stabilized.<sup>17</sup> On the other hand L-isoleucine and L-valine derivatives show only monotropic SmC behavior: a tertiary carbon linked to the asymmetric center introduces unfavorable steric factors and makes molecular arrangement difficult.

**Spontaneous Polarization.** The Ps values of all the compounds are gathered in Table II. We were unable to determine the real Ps value of compound I-3 because of the short range of its monotropic chiral phase. The crystallization avoided an accurate measurement of its ferroelectric properties (see Figure 1).

Figures 2-4 show the dependence of the spontaneous polarization against the temperature in series I-III, respectively. The plots Ps(*t*) show a typical shape for a first-order transition in the compounds in series III with a phase sequence Ch-SmC\*: There is a very marked increase in Ps values below the transition temperature, which reaches a saturation value in the four compounds (Figure 4). However the increase in the Ps value in the compounds

(17) Gray, G. W.; Goodby, J. W. *G. Smectic Liquid Crystals Textures and Structures*; Leonard Hill: Glasgow, 1984.

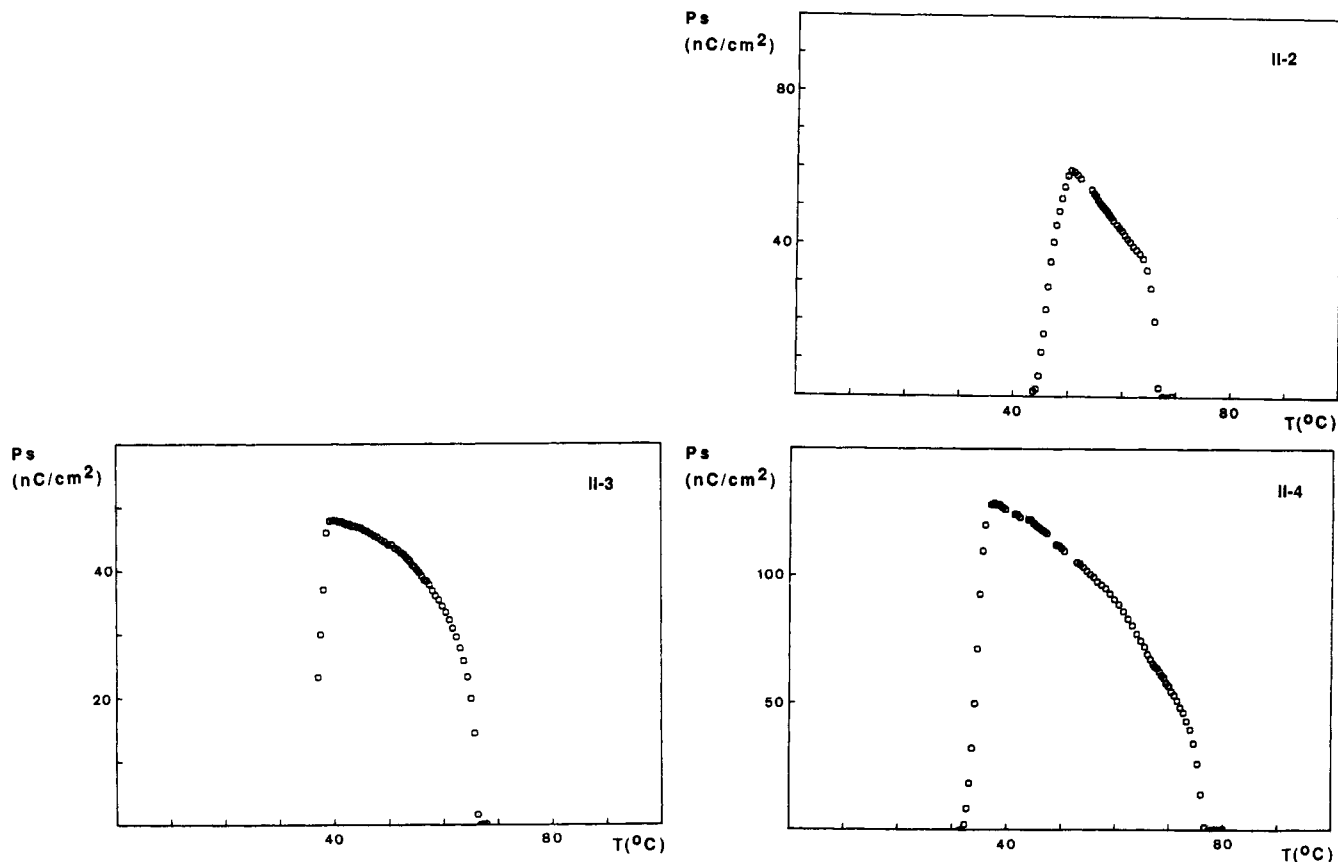


Figure 3. Temperature dependence of the polarization of the compounds in series II in the SmC\* phase.

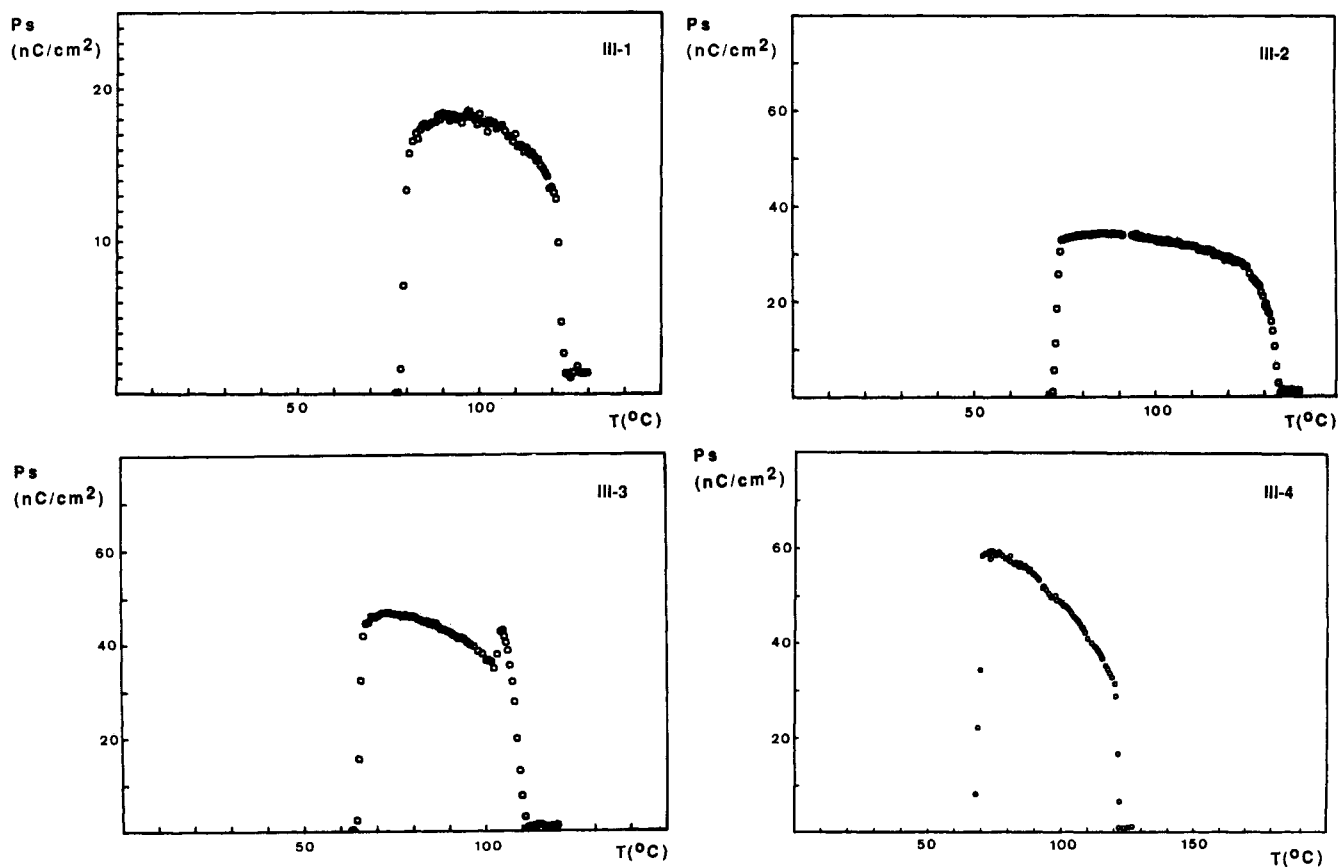
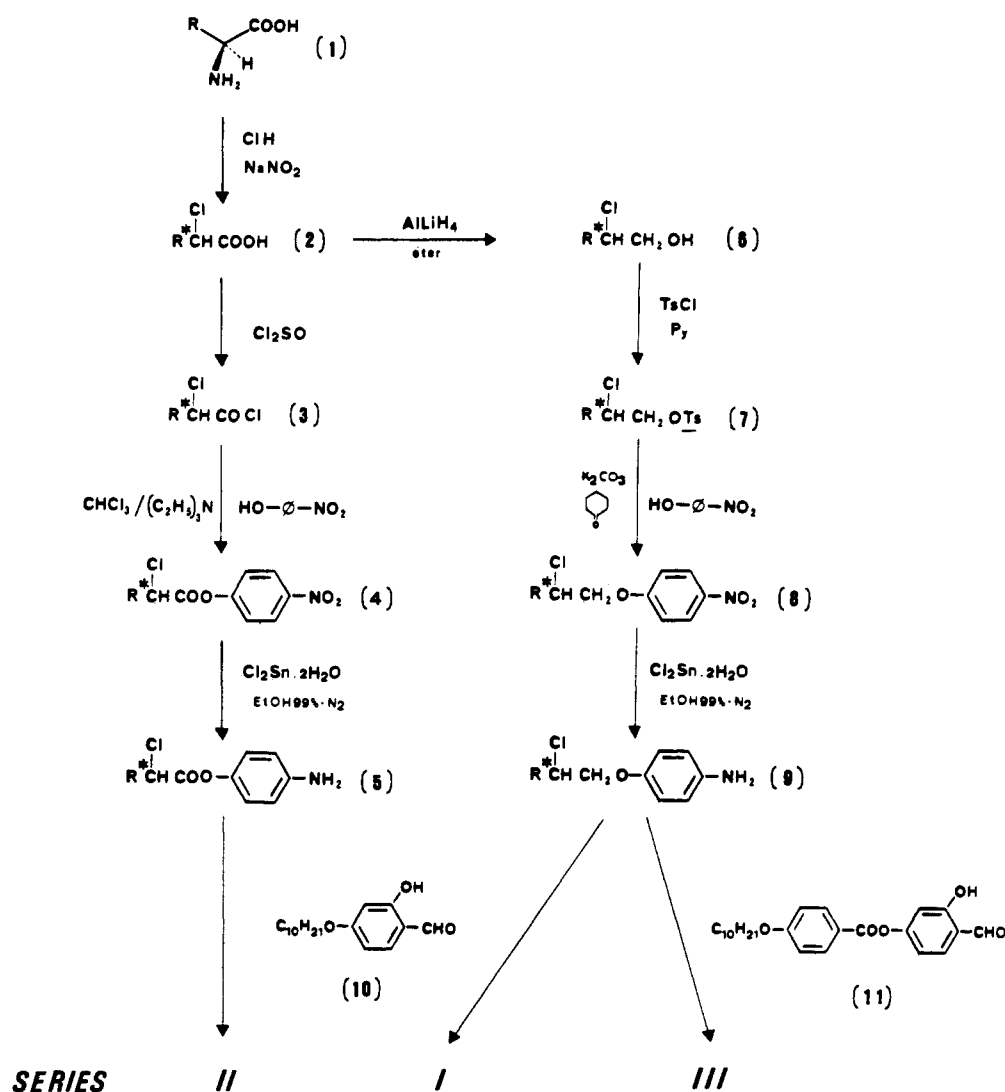


Figure 4. Temperature dependence of the polarization of the compounds in series III in the SmC\* phase.

in series I and II (Figures 2 and 3) is gradual when the temperature decreases. The second-order nature of the

transition SmA-SmC\* was corroborated by differential scanning calorimetry (DSC): The compounds in series I

Scheme I



show no peak in the transition temperature, which was determined by optical microscopy. In the compounds of series II, the transition  $\text{SmA-SmC}^*$  showed a peak, when the scanning rate was 10 and 5  $^\circ\text{C}/\text{min}$ , which disappeared at slower rates.<sup>18,19</sup>

A comparative study of the  $P_s$  values of series I and III with the same terminal tail indicates a slight influence of the core on  $P_s$  values. However, the compounds in series III have a third aromatic ring linked by an ester group. MNDO calculations of this structure showed the all-trans conformation as the most stable. In this way (see Figure 5) the partial dipole moment of the ester group strengthens the dipole associated with the chiral center. Nevertheless, the increase in the  $P_s$  values for compounds in series III is slight (even compound III-4 shows a smaller value). These results are not unexpected if we take into account the distance of this partial dipole moment from the asymmetric part of the molecule.

As far as the influence of the chiral tail is concerned, the compounds in series II with a carbonyl group adjacent to the chiral center show higher  $P_s$  values than their homologues in series I and III. The eight different chiral tails were studied by MM2 to obtain information about their most favored conformations. As a representative example,

Figure 6 shows the most abundant conformations obtained for (2*S*,3*S*)-2-chloro-3-methylpentanoyloxy and (2*S*,3*S*)-2-chloro-3-methylpentylloxy. The effect of the carbonyl group is 2-fold: In the first place the molecular dipole is increased by the interaction of both partial dipoles associated to  $\text{C}=\text{O}$  and  $\text{C}-\text{Cl}$  bonds. Second, the steric interaction of the oxygen and chlorine atoms decreases the rotating freedom in the chiral tail. This gives rise to a better coupling of the whole molecular structure with the asymmetric part of the molecule. Both factors, dipolar and steric, are responsible for the higher  $P_s$  values in compound derivatives of  $\alpha$ -chlorocarboxylic acids.

Another steric factor is the volume of the alkyl group in the chiral tail. The influence of this factor on the independent rotation of each molecule around its long axis is specially noteworthy. The closer the chiral center to the branching of the alkyl group, the bigger the hindrance to free rotation and the greater the intermolecular coupling of the dipole moments. The highest  $P_s$  values were found for the *L*-valine derivatives in the three series of compounds synthesized. Despite of having a *sec*-butyl group instead of an isopropyl group, the *L*-isoleucine derivatives show slightly lower  $P_s$  values in series II and III.

### Experimental Section

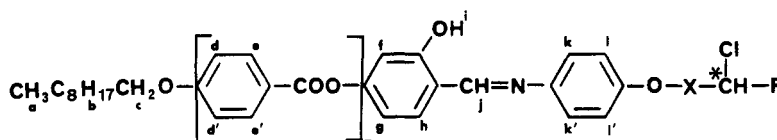
**Synthesis.** The full synthetic route is outlined in Scheme I. (i) **Synthesis of the Chiral Tails 2 and 6.** The chiral chains introduced in these compounds were all prepared from the cor-

(18) Bahr, C.; Heppke, G. *Mol. Cryst. Liq. Cryst.* 1987, 150B, 313.

(19) Heppke, G.; Löttsch, D.; Shashidhar, R. *Liq. Cryst.* 1989, 5(2), 489.

Table III. Elemental Analysis and the Most Relevant IR Data for the Compounds in the Series

compd	% C		% H		% N		$\nu_{C=O}$ , $\text{cm}^{-1}$	$\nu_{C=N}$ , $\text{cm}^{-1}$
	calc	exp	calc	exp	calc	exp		
I-1	70.03	70.62	8.08	8.51	3.14	3.37		1622
I-2	72.38	72.03	8.62	9.03	2.87	3.07		1626
I-3	72.38	71.82	8.62	9.02	2.87	3.00		1622
I-4	70.96	71.55	8.45	8.46	2.96	3.03		1622
II-1	67.90	68.35	7.40	7.89	3.05	2.94	1768	1616
II-2	69.39	69.87	7.98	7.73	2.79	2.84	1767	1616
II-3	69.39	69.56	7.98	8.40	2.79	2.82	1765	1614
II-4	68.92	69.41	7.79	8.20	2.87	3.00	1767	1614
III-1	70.03	70.54	7.07	7.52	2.48	2.65	1733 1719	1619
III-2	71.11	71.61	7.57	7.07	2.30	2.04	1733 1718	1620
III-3	71.11	71.29	7.57	7.95	2.30	2.21	1733 1718	1617

Table IV. 200-MHz Spectra of Compounds in Series I-III in  $\text{CDCl}_3^f$ (a) Central Core and Decyloxy Terminal Groups<sup>a-c</sup>

	a	b	c	dd'	ee'	f	g	h	i <sup>d</sup>	j	kk'	ll'
$n = 0$ , X = $\text{CH}_2$ (series I)	0.89 (t)	1.29-1.84 (m)	3.99 (t) $J = 6.3$	6.97 (d) $J = 8.6$	8.13 (d) $J = 8.6$	6.90 (d) $J = 2.4$	6.81 (dd) $J = 8.4, 2.4$	7.43 (d) $J = 8.4$	13.7 (s)	8.62 (s)	7.29 (d) $J = 8.5$	6.97 (D) $J = 8.5$
$n = 0$ , X = CO (series II)	0.89 (t)	1.29-1.84 (m)	3.99 (t) $J = 6.3$			6.45 (s)	6.47 (d) $J = 8.4$	7.23 (d) $J = 8.4$	13.8 (s)	8.50 (s)	7.23 (d) $J = 8.9$	6.93 (d) $J = 8.9$
$n = 1$ , X = $\text{CH}_2$ , (series III)	0.85 (t)	1.27-1.90 (m)	4.00 (t) $J = 6.5$			6.45 (s)	6.47 (d) $J = 8.4$	7.15 (d) $J = 8.4$	13.5 (s)	8.51 (s)	7.15 (m)	

(b) Chiral Terminal Chains<sup>c,e</sup>

	R = $\text{CH}_3$	R = $\text{CH}_2\text{CH}(\text{CH}_3)_2$	R = $\text{CH}(\text{CH}_3)\text{CH}_2\text{CH}_3$	R = $\text{CH}(\text{CH}_3)_2$
X = $\text{CH}_2$ (series I, III)	4.02-4.36 (m) 3 H 1.65 (d), 3 H, $J = 6.6$	4.05-4.30 (m), 3 H 1.83 (m), 2 H 1.29-1.80 (m), 1 H 0.99 (d), 3 H, $J = 6.6$ 0.96 (d), 3 H, $J = 6.6$	4.10-4.25 (m), 3 H 1.98 (m), 1 H 1.29-1.84 (m), 2 H 1.10 (d), 3 H, $J = 6.8$ 0.96 (t), 3 H, $J = 7.4$	4.10-4.20 (m), 3 H 2.18 (m), 1 H 1.08 (d), 2 H, $J = 6.6$ 1.11 (d), 3 H, $J = 6.6$
X = CO, (series II)	4.68 (c), 1 H, $J = 6.9$ 1.88 (d), 3 H, $J = 6.9$	4.50 (t), 1 H, $J = 7.0$ 2.00 (m), 2 H 1.28 (m), 1 H 1.15 (d), 3 H, $J = 6.8$ 0.99 (t), 3 H, $J = 7.3$	4.39 (d), 1 H, $J = 7.1$ 2.20 (m), 1 H 1.28 (m), 2 H 1.05 (d), 3 H, $J = 6.7$ 1.01 (d), 3 H, $J = 6.7$	4.35 (d), 1 H, $J = 6.7$ 2.40-2.60 (m), 1 H 1.17 (d), 6 H, $J = 6.8$

<sup>a</sup> These signals are practically identical ( $\pm 0.02$  ppm) for the four compounds in each series. <sup>b</sup> s, singlet; d, doublet; t, triplet; m, multiplet. <sup>c</sup> Coupling constants for first-order analysis. <sup>d</sup> Broad signal. <sup>e</sup> These signals are practically identical ( $\pm 0.03$  ppm) for the related compounds in series I and III. <sup>f</sup>  $\delta$  values in ppm;  $J$  values in hertz.

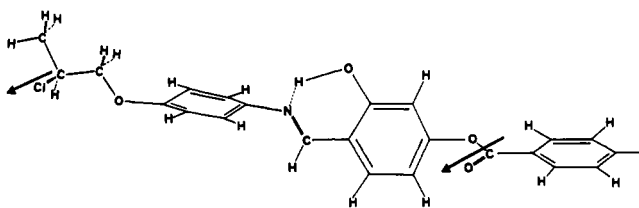


Figure 5. All-trans conformation of compound I-1 obtained by means of MNDO calculations.

responding commercial L- $\alpha$ -amino acids (1) readily available in high enantiomeric purity: L- $\alpha$ -alanine, L-leucine, and L-isoleucine, and L-valine. The  $\alpha$ -chloro acids (2) in series II were synthesized by means of a nucleophilic substitution of the amino group by a chlorine atom via the diazonium salt, as reported by Fu et al.<sup>20</sup> The substitution takes place with retention of the asymmetric center configuration.<sup>21</sup> Reduction of the acid group to alcohol, using  $\text{AlLiH}_4$  in dry ether as a reductor agent,<sup>22</sup> gave rise to the

corresponding  $\beta$ -chlorohydrins (6) of series I and III.

(ii) **Preparation of the Chiral Anilines 5 and 9.** The esterification of *p*-nitrophenol to obtain *p*-nitro(acyloxy)benzenes 4 was made via acid chloride 3 in  $\text{CHCl}_3/\text{Et}_3\text{N}$  with retention of asymmetrical configuration. The etherification of *p*-nitrophenol to obtain *p*-nitroalkoxybenzenes 8 was carried out via *p*-toluenesulfonate derivatives 7.<sup>23</sup> The alkylation reaction was carried out using  $\text{K}_2\text{CO}_3$  as a base and cyclohexanone as a solvent.<sup>24</sup> Chiral *p*-nitro(acyloxy)benzenes 4 and *p*-nitroalkoxybenzenes 8 were purified by flash chromatography using toluene and hexane/toluene (1/1), respectively, as eluents. Chiral anilines 5 and 9 were obtained by the reaction of each nitro analogue using the Bellamy method<sup>25</sup> with  $\text{SnCl}_2 \cdot 2\text{H}_2\text{O}$  in ethanol and under a  $\text{N}_2$  atmosphere. The amines obtained were used without further purification in the condensation step.

(iii) **Synthesis of Schiff Bases.** The 12 Schiff Bases were prepared by catalyzed condensation of the corresponding chiral anilines with the 4-(decyloxy)-2-hydroxybenzaldehyde (10, series I and II) and 4-(4'-(decyloxy)benzoyloxy)-2-hydroxybenzaldehyde (11, series III) in absolute ethanol. Schiff bases were purified by two recrystallizations from ethanol and hexane.

(20) Fu, S. C. J.; Birnbaum, S. M.; Greenstein, I. P. *J. Am. Chem. Soc.* 1954, 76, 6054.

(21) Faustini, F.; Demunari, S.; Panzeri, A.; Villa, V.; Gandolfi, C. *Tetrahedron Lett.* 1981, 22(45), 4533.

(22) Eliel, E. L. *J. Am. Chem. Soc.* 1978, 78, 1193.

(23) Dolphin, D.; Muljani, Z.; Cheng, J.; Meyer, R. B. *J. Chem. Phys.* 1973, 58, 413.

(24) Alabart, J. L.; Marcos, M.; Melendez, E.; Serrano, J. L. *Ferroelectrics* 1984, 58, 37.

(25) Bellamy, F. D.; Ou, K. *Tetrahedron Lett.* 1984, 25, 839.

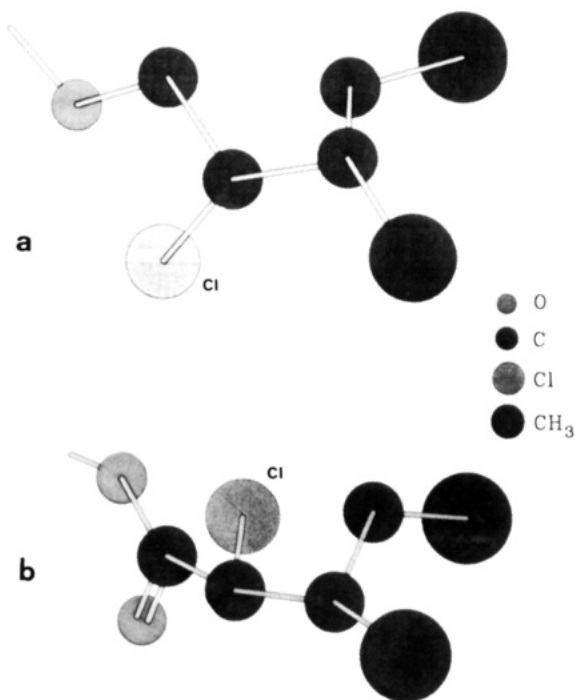


**Figure 6.** Most abundant conformations of chiral terminal chains for (2*S*,3*S*)-2-chloro-3-methylpentanoyloxy (a) and (2*S*,3*S*)-2-chloro-3-methylpentylloxy (b) obtained by means of MM2 calculations.

4-(Decyloxy)-2-hydroxybenzaldehyde (**10**) was prepared from the 2,4-dihydroxybenzaldehyde and  $C_{10}H_{21}Br$  by Williamson's method using  $KHCO_3$  as a base and acetone as a solvent.<sup>26</sup> 4-(4'-Decyloxy)benzoyloxy-2-hydroxybenzaldehyde (**11**) was obtained by esterification in  $CHCl_3/Et_3N$  of the 2,4-dihydroxybenzaldehyde with 4-(decyloxy)benzoyl chloride and further purification in flash chromatography using hexane/toluene (3/1) as eluent. 4-(Decyloxy)benzoyl chloride was prepared from commercially purchased 4-(decyloxy)benzoic acid.

**Characterization of the Schiff Bases.** Elemental analysis and the most relevant IR and UV-visible data of the final compounds are given in Table III. The  $^1H$  NMR data are gathered in Table IV.

**Optical Purity of the Compounds.** The optical purity was checked for the acids, the chlorhydrines, and the final compounds through the  $^1H$  NMR spectra of the *L*-isoleucine derivatives. The

presence of the second asymmetric carbon in the molecule gives rise to two diastereomeric compounds when there is a mixture of the *R* and *S* enantiomers in the asymmetric carbon with the chlorine atom. In this case, two signals were observed for the hydrogen belonging to this carbon atom. None of the *L*-isoleucine derivatives show peaks due to the presence of diastereoisomers. We have assumed that as the synthetic process is the same, all the compounds behave similarly as far as optical purity is concerned.

**Techniques.** Microanalysis was performed with a Perkin-Elmer 240 B microanalyzer. Infrared spectra for all the compounds were obtained by using a Perkin-Elmer 1600 (series FTIR) spectrometer using Nujol mulls between polyethylene plates in the 360–4000- $cm^{-1}$  spectral range. The UV-visible spectra for the compounds were recorded in cyclohexane by using a Hitachi V-3400 spectrophotometer in the 200–500-nm spectral range.  $^1H$  NMR spectra were recorded on a Varian XL-200 spectrometer operating at 200 MHz for  $^1H$  in deuteriochloroform solutions. The textures of the mesophases were studied with a Nikon optical microscope equipped with a polarizing light, a Mettler FP82 hot stage, and a Mettler FP80 central processor.

Measurements of temperatures and enthalpies of transition were carried out using a Perkin-Elmer DSC-7 differential scanning calorimeter with a heating and cooling rate of 10  $^{\circ}C/min$  (the apparatus was calibrated with indium, 156.6  $^{\circ}C$ , 28.44 J/g) and tin (232.1  $^{\circ}C$ , 60.5 J/g).

## Conclusions

A significant increase in the  $P_s$  values with no modification of mesogenic behavior is observed in the derivatives of  $\alpha$ -chloro acids (series II) compared with their homologous  $\beta$ -chlorohydrine derivatives (series I).

In the case of the  $\beta$ -chlorohydrine tails, the third aromatic ring in the compounds in series III gave rise to a considerable increase in the stability of the SmC\* phase related to the compounds in series I. However, the  $P_s$  values were not influenced to such a noticeable degree and are only slightly higher in three of the compounds and lower for the derivative of *L*-valine (4-(4'-(decyloxy)benzoyloxy)-2-hydroxybenzilidene-4'-(2*S*-2-chloro-3-methylbutanoyloxy)aniline, III-4).

**Acknowledgment.** We thank Drs. A. M. Levelut and J. Barberá, who carried out the X-ray measurements in the Laboratoire de Physique des Solides, Orsay, France. This work was financed by the CICYT (Project MAT-88-324-CO2-01).

**Registry No.** I-1, 131010-80-5; I-2, 131010-81-6; I-3, 131010-82-7; I-4, 131010-83-8; II-1, 131010-84-9; II-2, 131010-85-0; II-3, 131010-86-1; II-4, 131010-87-2; III-1, 131010-88-3; III-2, 131010-89-4; III-3, 131010-90-7; III-4, 131010-91-8.

(26) Artigas, M.; Marcos, M.; Melendez, E.; Serrano, J. L. *Mol. Cryst. Liq. Cryst.* **1985**, *130*, 337.